Received: 1 September 2021 | Accepted: 8 February 2022

DOI: 10.1111/imb.12766

ORIGINAL ARTICLE

Insect Molecular Biology

GrpE is involved in mitochondrial function and is an effective target for RNAi-mediated pest and arbovirus control

Yan Huo[1,2] | Zhiyu Song[1,2] | Haiting Wang[1,2,3] | Ziyu Zhang[4] | Na Xiao[1,2] | Rongxiang Fang[1,2] | Yuman Zhang[1,2] | Lili Zhang[1,2]

[1]State Key Laboratory of Plant Genomics, Institute of Microbiology, Chinese Academy of Sciences, Beijing, China

[2]CAS Center for Excellence in Biotic Interactions, University of Chinese Academy of Sciences, Beijing, China

[3]University of the Chinese Academy of Sciences, Beijing, China

[4]College of Life Sciences, Hebei University, Baoding, China

Correspondence
Lili Zhang and Lili Zhang, Institute of Microbiology, Chinese Academy of Sciences, No 3, Yard 1, West Beichen Road, Chaoyang, Beijing 100101, China.
Email: zhangll@im.ac.cn and zhangym@im.ac.cn

Funding information
National Key Research and Development Program of China, Grant/Award Number: 2019YFC1200503; Strategic Priority Research Program of Chinese Academy of Sciences, Grant/Award Number: XDPB16; Youth Innovation Promotion Association of the Chinese Academy of Sciences, Grant/Award Number: 2021084

Abstract

Laodelphax striatellus is a sap-feeding pest and the main insect vector of *rice stripe virus* (RSV). There is an urgent need to identify molecular targets to control this insect pest and plant arboviruses. In this study, we identified a *L. striatellus* gene (named *LsGrpE*) encoding a GroP-E-like protein. We found that the LsGrpE protein localized to mitochondria. Using gene-specific dsRNA to interfere with the expression of *LsGrpE* led to a significant increase in insect mortality, and most of the surviving insects could not develop into adults. Further analyses revealed that *LsGrpE* deficiency caused mitochondrial dysfunction and inhibited the insulin pathway, resulting in diabetes-like symptoms such as elevated blood sugar, inactive behaviour, developmental delay, and death. In addition, *LsGrpE* deficiency significantly reduced the RSV titre in surviving *L. striatellus*, and indirectly prevented viral vertical transmission by reducing the number of adults. We generated transgenic rice plants expressing *LsGrpE*-specific dsRNA, and the dsRNA was acquired by *L. striatellus* during feeding, resulting in increased insect mortality and the prevention of arboviral transmission. This study clarifies the function of LsGrpE and demonstrates that LsGrpE can be used as a molecular target of plant-generated dsRNA to resist this sap-feeding pest, a17nd therefore, its transmitted arboviruses.

KEYWORDS
GroP-like gene E, insect resistant, insulin pathway, *Laodelphax striatellus*, mitochondria dysfunction, *rice stripe virus*

INTRODUCTION

The Homoptera species *Laodelphax striatellus* (small brown planthopper, SBPH) is one of the most widespread pests in East Asian agriculture and causes losses of millions of dollars every year (Liu et al., 2006). During feeding, these insects transmit various plant viruses, such as *rice stripe virus* (RSV). RSV is a persistent-propagative virus transmitted by SBPH, and its vertical transmission, mediated by the insect vitellogenin transport pathway, has led to an increase in the population of RSV-infected insects, thereby increasing rice stripe disease outbreaks (Huo et al., 2014; Huo et al., 2018; Huo et al., 2019). Many plant viruses are transmitted via insect feeding, including plant arboviruses that cause large economic losses (Hogenhout et al., 2008). Because traditional chemical pesticides can pollute the environment and lead to insect resistance, it is important to develop effective, green methods for preventing pests and controlling plant arboviruses. Previous research has identified several effective insect-resistance factors that can be used for applications in agriculture. For decades, heterologous insecticidal proteins such as insecticidal crystal proteins and vegetative insecticidal protein (Vip) derived from *Bacillus thuringiensis* Bt, have been exploited to produce

Yan Huo and Zhiyu Song are contributed equally to this study.

crop lines resistant to chewing insects (Bakhsh et al., 2020; Makkar et al., 2019). This has led to the rapid and large-scale production of transgenic crops (e.g., cotton, potato) resistant to chewing pests. More recently, transgenic plants that resist sap-feeding pests (planthopper, aphid, thrip, whitefly) have also been developed (Bhattacharya, 2019; Guo et al., 2013; Han et al., 2019; Kim et al., 2019; Xia et al., 2021; Zhang et al., 2015). The current research aims to identify more target genes with roles in defence against sap-feeding pests and their transmitted arboviruses.

GroP-like E (GrpE) is a co-chaperone of Hsp70 that functions as a nucleotide exchange factor (NEF), and is widely found in prokaryotes and in the mitochondria/chloroplasts of eukaryotic organisms (Melero et al., 2015). Mitochondrial GrpE (mtGrpE) is synthesized outside of the mitochondria and imported inside via its specific mitochondrial targeting peptide (mTP) (Langner et al., 2014). Inside the mitochondrial matrix, the mtGrpE dimer binds to Hsp70 to activate the chaperone system by nucleotide exchange (Konovalova et al., 2018; Marada et al., 2013). The chaperone system inside the mitochondria is essential for maintaining mitochondrial protein quality by folding the freshly-imported proteins and refolding the defective proteins. Disrupting the chaperone system in the mitochondria disrupts protein homeostasis, which on the one hand, results in the accumulation of misfolded proteins and the activation of protective genes that regulate protein homeostasis in the nucleus (Fang et al., 2017; Hartl et al., 2011; Yoneda et al., 2004), but on the other hand, can trigger mitochondrial dysfunction (mtD) (Coyne & Chen, 2019; Mottis et al., 2014).

The mitochondria of eukaryotic cells are the energy centres that produce ATP and eliminate reactive oxygen species (ROS). Dysfunction of these organelles usually leads to energy deficiency and excessive ROS (Clavier et al., 2016; Pfanner et al., 2019). The accumulation of ROS causes aging, metabolic disorders, hypoevolutism, and even death (Jing et al., 2011; Nunnari & Suomalainen, 2012; Sebastián et al., 2012; Wang & Wei, 2020). Excessive levels of ROS can also downregulate sugar transporters by disrupting insulin signal transduction, leading to insulin resistance (Jing et al., 2011; Lantier et al., 2015). For example, Hsp60 deficiency in mice causes mtD and induces insulin resistance and diabetes (Kleinridders et al., 2013). The GrpE homologue of *Saccharomyces cerevisiae*, Mge1, responds to oxidative stress to protect protein homeostasis in the mitochondria (Marada et al., 2013). Disruption of the Mge1-Hsp70 complex makes cells more susceptible to H_2O_2, while the more stable Mge1-Hsp70 complex makes cells resistant to oxidative stress (Marada et al., 2013).

In this study, we identified a single copy GrpE homologue from the *L. striatellus* genome and designated the protein as *L. striatellus* GrpE (LsGrpE). LsGrpE localized to the mitochondria in *L. striatellus*. Knockdown of *LsGrpE* expression caused mtD-induced saccharometabolic disorders by interfering with the insulin pathway. LsGrpE deficiency also led to inert movement, developmental delays, and the death of *L. striatellus*. The RSV titre was significantly decreased in LsGrpE-deficient viruliferous *L. striatellus*. Based on the critical role of LsGrpE in *L. striatellus* and RSV transmission, we used RNA interference (RNAi) technology to overexpress double-stranded RNA (dsRNA) targeting *LsGrpE* in rice (*Oryza sativa*). Transgenic rice plants showed remarkable resistance to this sap-feeding pest, as well as to its arboviruses. These results demonstrate an effective target gene with an important application in the control of sucking pests.

RESULTS

L. striatellus GrpE is a mitochondrial protein

The GrpE homologue was initially identified from a yeast surface-displayed *L. striatellus* cDNA library. By alignment with the *L. striatellus* genome (Zhu et al., 2017), we obtained the full sequence of *GrpE* and found that it exists in single copy in the *L. striatellus* genome. Therefore, we named the gene *L. striatellus GrpE* (*LsGrpE*).

Sequence analyses revealed that *LsGrpE* contains an open reading frame of 705 base pairs, encoding a polypeptide of 234 amino acids (Figure 1a). The subcellular localization of LsGrpE was predicted by the TargetP-1.1 server (https://services.healthtech.dtu.dk/service.php?TargetP-1.1). There is a 45-amino acid mTP at the N-terminus of LsGrpE (Figure 1a), suggesting that LsGrpE may be a mitochondrial protein. After removing the mTP, the estimated molecular weight was 22 kDa. By phylogenetic analyses, the GrpE homologues were assigned to six groups, including homologues from arthropod mitochondria, vertebrate mitochondria, plant mitochondria, fungi, bacteria, and plant chloroplasts. LsGrpE showed the highest similarity to the arthropod mitochondrial GrpEs (Figure 1b).

To investigate whether LsGrpE localized in mitochondria, mitochondria were separated from the cytoplasm. A mitochondria-specific probe (Mito-Tracker) was used to indicate the mitochondria. The Mito-Tracker signal was observed in the samples corresponding to whole-cell homogenates and extracted mitochondria but not the cytoplasmic samples, indicating effective separation of mitochondria and cytoplasm (Figure 2a). The proteins extracted from the isolated mitochondria and cytoplasm were subjected to western blot analyses using LsGrpE-specific antibodies. A strong 22 kDa band hybridized to the LsGrpE-specific antibodies in the total protein sample and the mitochondrial sample, but not in the cytoplasmic sample (Figure 2b), indicating that LsGrpE is a mitochondrial protein. The 27 kDa full-length protein could not be detected by western blotting of the total protein or cytoplasmic samples, suggesting that most of the protein was localized to the mitochondria. We performed a gene knockdown experiment to confirm the specificity of the LsGrpE antibodies. After the level of *LsGrpE* mRNA was reduced by *LsGrpE*-specific double-stranded RNA (dsLsGrpE), western blotting of LsGrpE revealed a significantly weaker band (Figure 2c,d).

LsGrpE is important for the survival and development of *L. striatellus*

To investigate the function of LsGrpE, 3rd instar larvae were injected with ds*LsGrpE*, then fed on healthy rice seedlings for 3 weeks. The insects' development and mortality were recorded daily. Starting from 2 days post-microinjection (dpi), the mRNA level

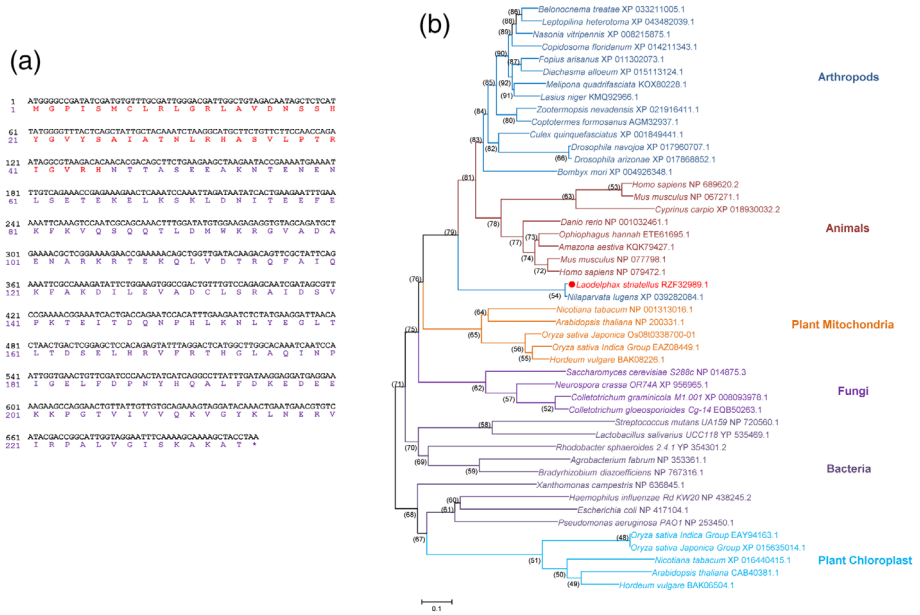

FIGURE 1 Phylogenetic analyses of proteins homologous to LsGrpE. (a) Nucleotide and predicted amino acid sequences of LsGrpE. Red colour indicates the mitochondrial targeting peptide predicted by the TargetP 1–1 server. (b) Phylogenetic analyses of the LsGrpE protein sequence and homologues from arthropods, animals, fungi, bacteria and plants, and. A total of 47 GrpE homologues were aligned and analysed using the neighbour-joining method by the software MEGA 6

of *LsGrpE* was significantly reduced by the gene-specific dsRNA (Figure 3a). Compared with insects injected with the ds*GFP* negative control, the ds*LsGrpE*-treated insects showed higher mortality. From 8 dpi, mortality was significantly higher in the ds*LsGrpE* group than in the ds*GFP* group. On 15 dpi, less than 50% of the ds*LsGrpE*-injected *L. striatellus* survived, while the survival rate of the control group was 90% (Figure 3b). These results indicated the importance of LsGrpE for insect survival.

L. striatellus belongs to the order Homoptera and undergoes five larval stages before reaching adulthood. Generally, every 5–7 days, insects moult and move to the next stage as they develop into adults. We detected that at 12 dpi, insects in the control group gradually moulted and became adults. At the end of the experiments, all of the control-group insects became adults. By comparison, an average of 10% of the surviving *LsGrpE*-deficient insects moulted and became adults, the remaining 90% stayed in the larval state and did not moult into adults before death (Figure 3c). These results indicated that LsGrpE-deficiency interfered with the development of *L. striatellus*.

We also compared the insects' physiological condition. Insects in the control group displayed vigorous activity and fed on the whole plant. By contrast, the *LsGrpE*-deficient insects were weak, moved slowly, and remained at the bottom of the plant when feeding (Figure 3d). To confirm the inactive behaviour induced by LsGrpE deficiency, we measured the time taken for insects to reach food (i.e., rice seedlings). Both *dsLsGrpE*-treated insects and *dsGFP*-treated control insects were placed at the same distance (3 cm) from the rice plant, then the time taken for the insects to reach the plants was recorded. Compared with the control insects, the *dsLsGrpE*-deficient insects took significantly more time to reach the plant (Figure 3e).

On the basis of the mitochondrial localization of LsGrpE, the inactive behaviour of insects, and the pre-moulting death caused by LsGrpE deficiency, we speculated that LsGrpE is involved in mitochondrial function and the supply of energy.

LsGrpE deficiency causes mtD

To test whether LsGrpE is essential for mitochondrial function, the gene was silenced by dsRNA microinjection, and the concentrations of ATP and ROS, which are indicators of mitochondrial activity, were determined at 7 dpi. Compared with insects in the control group, ds*LsGrpE*-deficient insects showed a significant reduction in ATP concentration (Figure 4a). The ROS in the gut and fat body were detected using fluorescent probes, which are oxidized by ROS to release fluorescent signals. Under normal circumstances, ROS in cells will be eliminated by mitochondria. In these analyses, ds*GFP*-treated insects showed weak fluorescent signals, while strong fluorescent signals were detected in the gut and fat body of the LsGrpE-deficient insects, indicating an excess of ROS resulting from LsGrpE deficiency (Figure 4b). These results confirmed that LsGrpE deficiency caused mtD.

Transcriptome sequencing of the LsGrpE knockdown and control insects also supported the role of LsGrpE in maintaining normal mitochondrial function. Comparison of the dsLsGrpE-treated and dsGFP-treated RSV-free insects revealed a significant change in the mRNA expression levels of 164 genes (Table S1). Among these 164 genes, at least 17 genes contained the mTP (Table S2), including the genes encoding inositol oxygenase, peptide methionine sulfoxide reductase, calcium signal-modulating cyclophilin ligand (CAML), and the

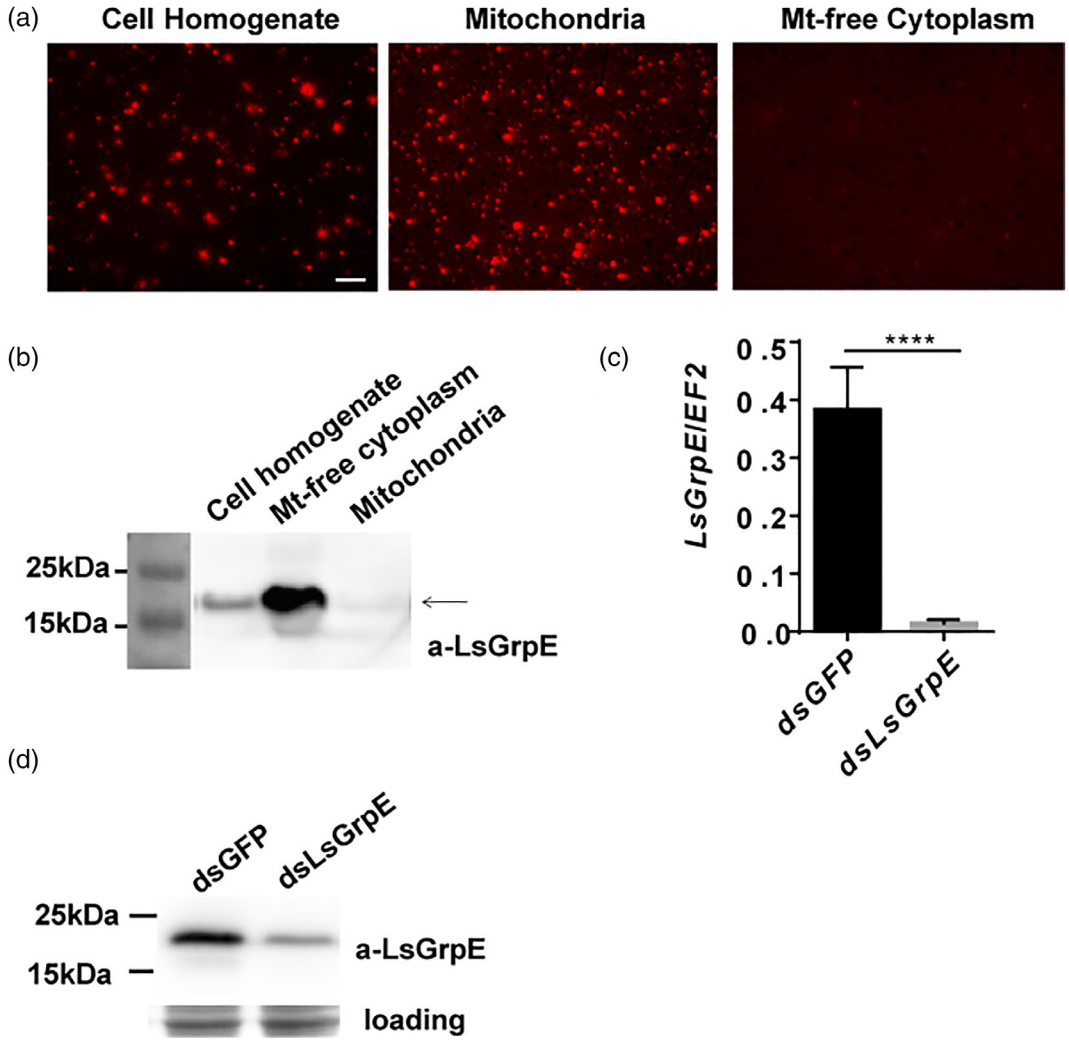

FIGURE 2 Mitochondrial localization of LsGrpE in *Laodelphax striatellus*. (a) Immunofluorescence microscopy to indicate the separated mitochondria. Mitochondria in the whole cell homogenate (Cell homogenate) and mitochondrial samples (Mitochondria) were stained red by Mito-tracker Red CMXRos, while the cytoplasm samples (Mt-free cytoplasm) were not stained. Bar = 10 μm. (b) Western blots to detect the LsGrpE proteins inside *L. striatellus*. LsGrpE-specific antibodies were used to detect LsGrpE. Arrow indicates the LsGrpE protein of 22 kDa. (c) D. Q-RT-PCR and western blots to show the antibody specificity. When the mRNA level of *LsGrpE* was reduced by dsLsGrpE (C), the protein level was also reduced (d). Insects were collected at 7 days post-dsRNA injection. Mean and SDs were calculated from three independent dsRNA injections, with four mRNA samples per experiment. ****, $p < 0.0001$

transcription factor of kayak isoform (TFKI). There were a number of other genes required for normal mitochondrial function or the response to mtD, which included the genes encoding the riboflavin transporter (RFT) required for riboflavin transportation, and the glutathione-specific gamma-glutamylcyclotransferase (GGCT) and its transcription factor gene CCAAT enhancer-binding protein (CEBPβ) regulating intracellular redox homeostasis in response to excess ROS. Gene ontology (GO) term enrichment analyses ($q < 0.05$) were performed to further understand the function of the differentially expressed genes (DEGs). A directed acyclic graph (DAG) showed the enrichment analyses results. In LsGrpE-deficient insects, the oxidoreductase activities ($q = 0.006$), monooxygenase activity ($q = 0.006$), and tetrapyrrole binding ($q < 0.001$) were highly enriched in molecular function (Figure S1).

Q-RT-PCR further confirmed the inducible expression of the mtD-related genes by LsGrpE knockdown (Figure 4c–i). Among these genes, *RFT*, *CAML*, and *TFKI* are related to mitochondrial respiratory function and ATP synthesis (Figure 4c–e), and their induced expression is consistent with the observed reduction in ATP production and the inactive behaviour (Figures 3b and 4a). *GGCT* and *CEBP*β regulate intracellular redox homeostasis in response to excess ROS (Figure 4f,g).

LsGrpE deficiency induces saccharometabolism disorders

The insulin/insulin-like growth factor (IGF) signalling (IIS) pathway plays a vital role in regulating glucose homeostasis in animals,

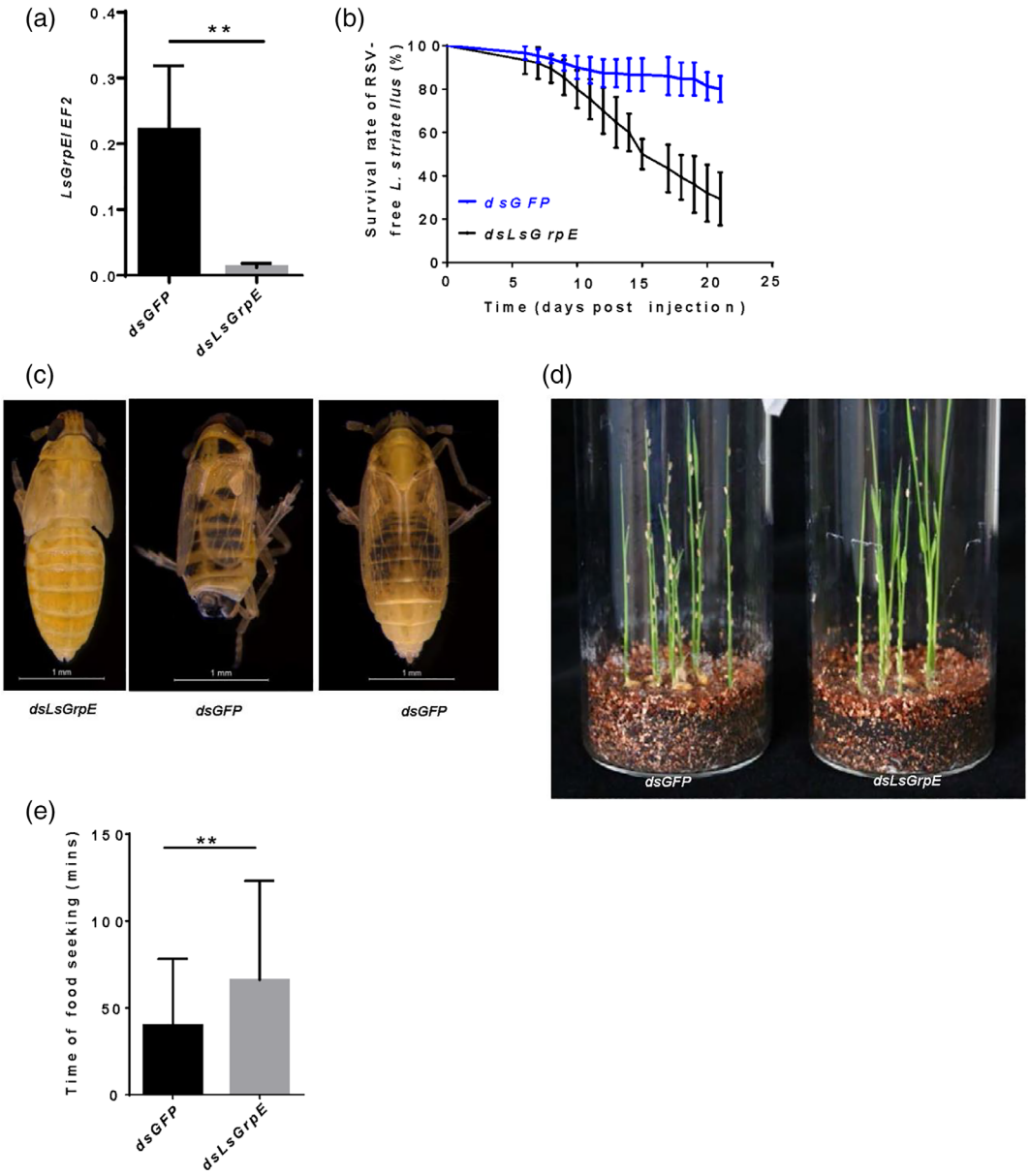

FIGURE 3 Effects of LsGrpE deficiency on *L. striatellus*. (a) Q-RT-PCR to confirm the knockdown of *LsGrpE* mRNA by ds*LsGrpE* injection. Insects at 2 dpi were used. Ds*GFP* served as a negative control. The mean and SD were calculated from three independent dsRNA injections, with six insects per experiment. **, $p < 0.01$. (b) Survival curves to show the effect of LsGrpE deficiency on insect survival. (c) Images showing the delayed development of LsGrpE-deficient *L. striatellus*. The three images represent 20 insects per group from four independently repeated dsRNA treatment experiments. From left to right, dsLsGrpE-treated insects arrested at the 5th larval stage, adult males and adult females from the control group. (d) Comparison of the behaviours of ds*LsGrpE*-treated and control insects. Insects were analysed at 3 dpi. (e) Comparison of the time taken to seek food. *L. striatellus* injected with dsGFP or dsLsGrpE were placed 3 cm away from rice seedlings. The seeking time of the first 15 insects in each group was recorded. The mean ± SD were calculated from three independent dsRNA injections, with 15 insects per experiment. **, $p < 0.01$

ranging from insects to mammals. It has been reported that in mammals and fruit flies, mtD interferes with the IIS pathway and induces insulin resistance and diabetes (Kleinridders et al., 2013; Maechler & Wollheim, 2000). Transcriptome analyses also showed that the gene encoding the negative regulator of IIS in *Drosophila*, imaginal morphogenesis protein-Late 2 (LsImpL2), was significantly upregulated under LsGrpE deficiency. Therefore, we investigated the possibility that LsGrpE deficiency causes sugar metabolism disorders through negative regulation of the insulin pathway.

Through qRT-PCR, we confirmed a four-fold increase in the mRNA level of *ImpL2* in LsGrpE-silenced *L. striatellus* (Figure 5a). We measured the expression of other IIS genes and found that after injection of ds*LsGrpE*, the transcript levels of key genes in IIS, including those encoding insulin-peptide 1 (IS1), insulin-peptide 3 (IS3), insulin-peptide receptor 1 (ISR1), and insulin-peptide receptor 2 (ISR2), were

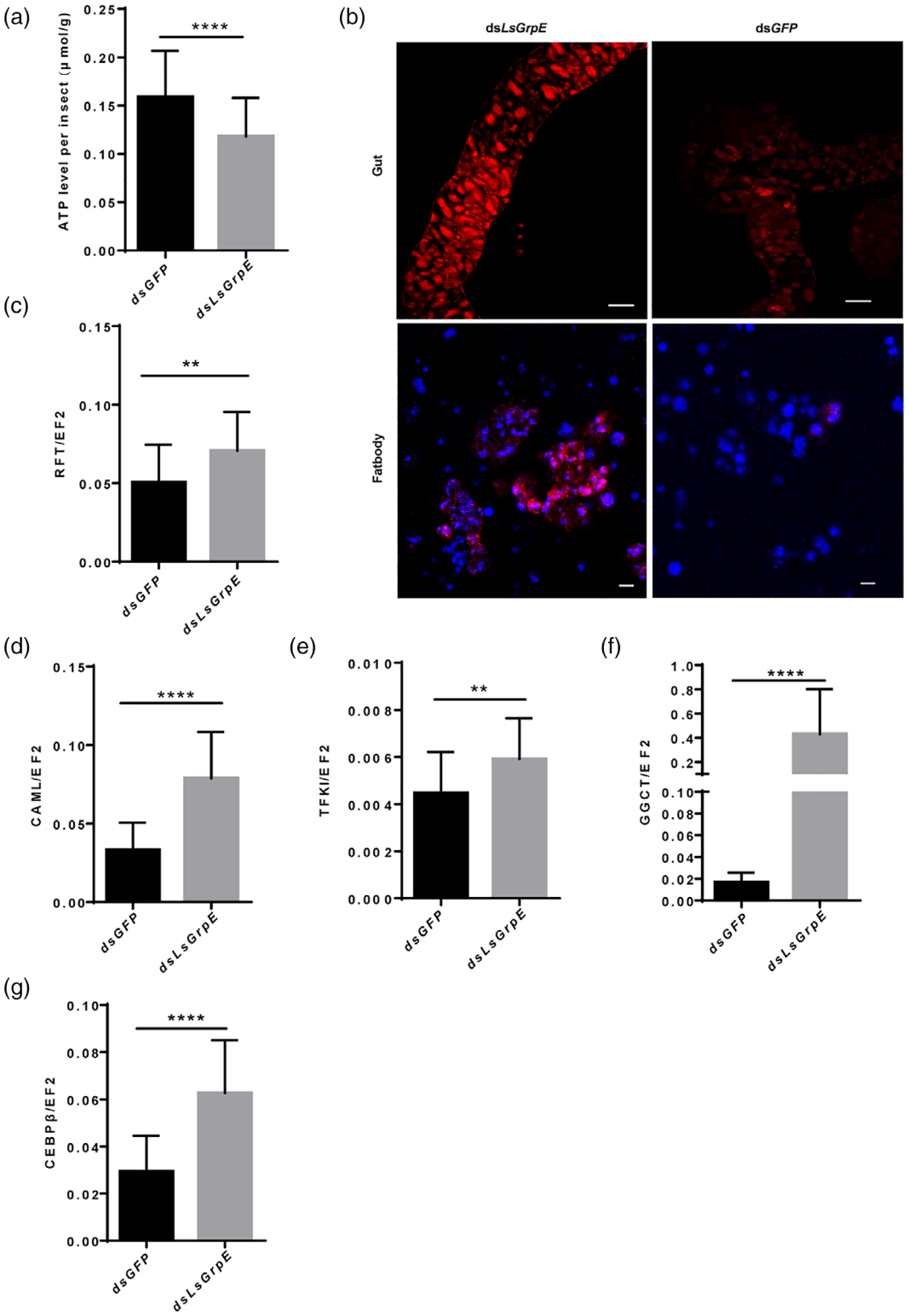

FIGURE 4 LsGrpE deficiency causes mitochondrial dysfunction. (a) ATP content assay on 7 dpi. The ATP contents (μmol/g) were quantitatively detected by measuring the change in absorbance at 340 nm, and the ATP contents of the samples were calculated by comparison with the standard sample. A total of six biological replicates were performed, each of which included three technical replicates. ***, $p < 0.001$. (b) Reactive oxygen species assay on 7 dpi. The gut and fatbody were stained with dihydroethidium (DHE). Red signals appeared in the presence of ROS. The signal intensity was related to the ROS level. Nuclei were stained with Hoechst 33342 (shown in blue). Bars relating to the gut and fatbody are 100 μm and 10 μm, respectively. (c–g) Q-RT-PCR to show the mRNA levels of the mtUPR-related genes. RFT, riboflavin transporter; CAML, calcium signal-modulating cyclophilin ligand; GGCT, glutathione-specific gamma-glutamylcyclotransferase; CEBPβ, transcription factor named as CCAAT enhancer-binding protein; TFKI, transcription factor of kayak isoform. The mean and SD were calculated from six biological replicates (one insect per replicate) with three technical replicates. *, $p < 0.05$, **, $p < 0.01$, ***, $p < 0.001$, ****, $p < 0.0001$

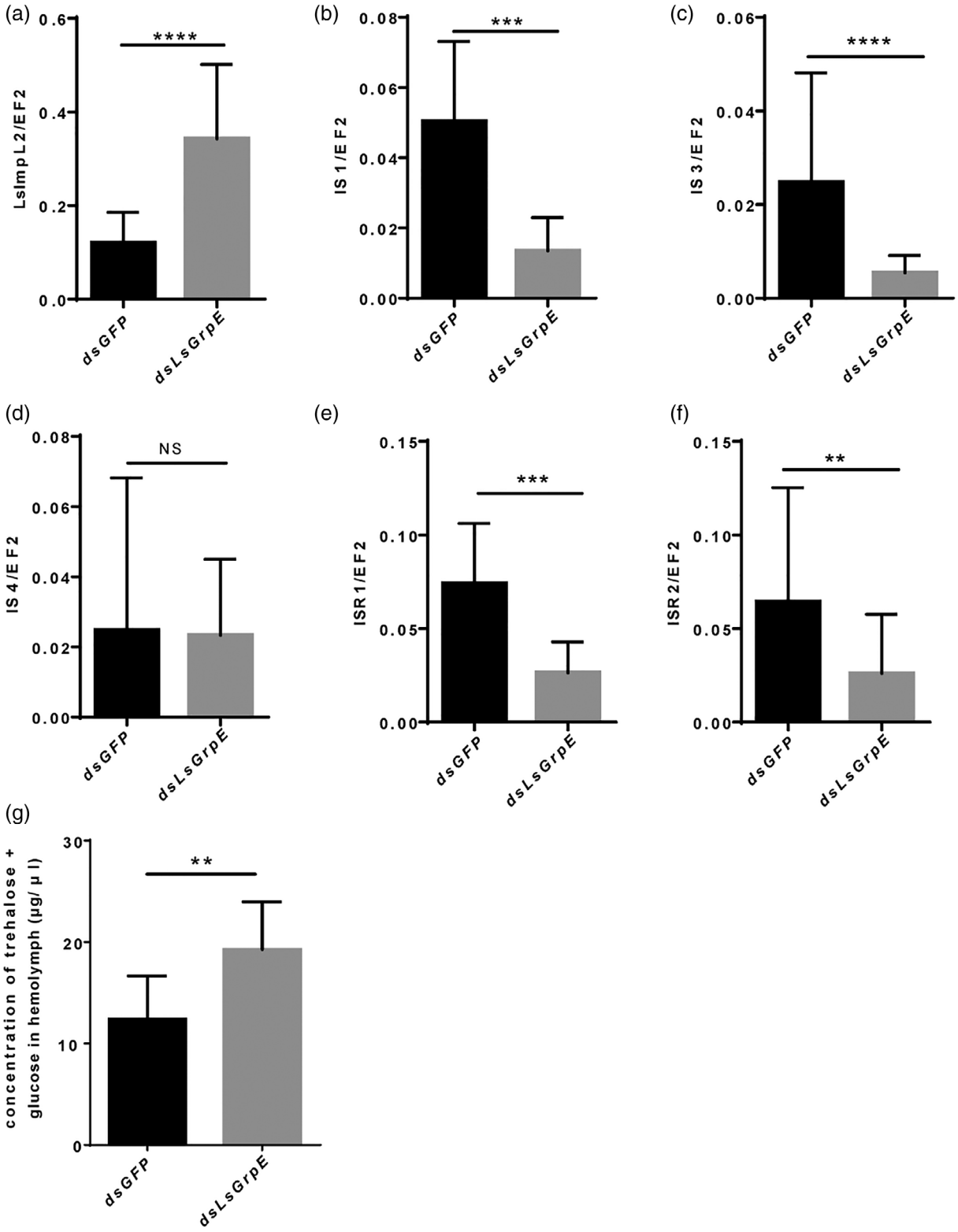

FIGURE 5 LsGrpE deficiency disturbs sugar metabolism. (a–f) IIS-related genes at 7 dpi. IS1, insulin-peptide 1; IS3, insulin-peptide 3; IS4, insulin-peptide 4; ISR1, insulin-peptide receptor 1; ISR2, insulin-peptide receptor 2; LsImpL2, *L. striatellus* imaginal morphogenesis protein-Late 2. (g) Concentration of the monoglysaccharides in haemolymph on 7 dpi. The mean and SD were calculated from six biological replicates (one insect per replicate) with three technical replicates. **, $p < 0.01$, ***, $p < 0.001$, ****, $p < 0.0001$, NS, not significant

significantly reduced, although that of the gene encoding insulin-peptide 4 (IS4) was unaffected (Figure 5b–f).

Then, we measured the circulating sugar content (trehalose plus glucose) in the LsGrpE-deficient and control *L. striatellus*. We found that at 7 dpi, the blood sugar level was higher in the ds*LsGrpE*-treated insects (19.3 ± 1.298 μg/μL) than in the control group (12.4 ± 1.418 μg/μL).

Collectively, these results indicated that LsGrpE deficiency interfered with the insulin pathway and caused mtD-induced saccharometabolic disorders.

LsGrpE deficiency reduced the RSV titre in *L. striatellus*

L. striatellus is the main insect vector of RSV. To test whether silencing of LsGrpE affects the RSV titre, the *LsGrpE* gene-specific dsRNA was delivered into RSV-infected 3rd instar larvae to block *LsGrpE* expression. At 7 dpi, the gene silencing efficiency was measured by q-RT-PCR analyses. Compared with ds*GFP* treatment, ds*LsGrpE* treatment decreased the *LsGrpE* mRNA level by 90%, indicating effective knockdown of *LsGrpE* (Figure 6a). Compared with control insects, the *LsGrpE*-deficient insects showed significantly higher mortality from 8 dpi onwards (Figure 6b). Next, q-RT-PCR analyses of RSV titres in the surviving *L. striatellus* at 7, 10, 13, 16, 19, and 21 dpi revealed much lower RSV titres in the *LsGrpE*-deficient insects than in control insects from 10 dpi onwards. The difference in viral titre between control and *LsGrpE*-deficient insects became larger over time, and reached the level of significance at 16 dpi (Figure 6c). Thus, *LsGrpE* deficiency negatively affected the RSV titre in *L. striatellus*.

LsGrpE-RNAi transgenic rice deters *L. striatellus* feeding and prevents RSV transmission

Having confirmed that dsLsGrpE interferes with the development and survival of *L. striatellus*, we then investigated whether *dsLsGrpE* could be expressed *in planta* to control the sap-feeding pests and arboviruses. It is known that dsRNA is cleaved into 21–24 nt siRNAs in plant cells. Considering the safety of transgenic plants, we analysed the degree of similarity in the LsGrpE sequence between the human (taxid: 9606), Japonica rice (taxid: 39947), cow (taxid: 9913), sheep (taxid: 9940) and leafhopper (taxid: 30102) genomes, and confirmed that there is no target for *LsGrpE* siRNA in these animals or insects. Then, we created transgenic rice plants over-expressing the LsGrpE-hairpin-RNA target (GP1, Figure 7a). We expected that *LsGrpE* siRNA would be acquired by insects during feeding and then silence the expression of *LsGrpE*. We evaluated the resistance of the transgenic rice lines to *L. striatellus* attack. The survival rate of *L. striatellus* feeding on transgenic plant lines was evaluated, and two effective lines, GP1-5, and GP1-1, were selected for further analyses (Figure S2). Line GP1-2 is also effective in resisting insects; however, there were insufficient seeds from GP1-2 for further experiments. Viruliferous *L. striatellus* were allowed to feed on

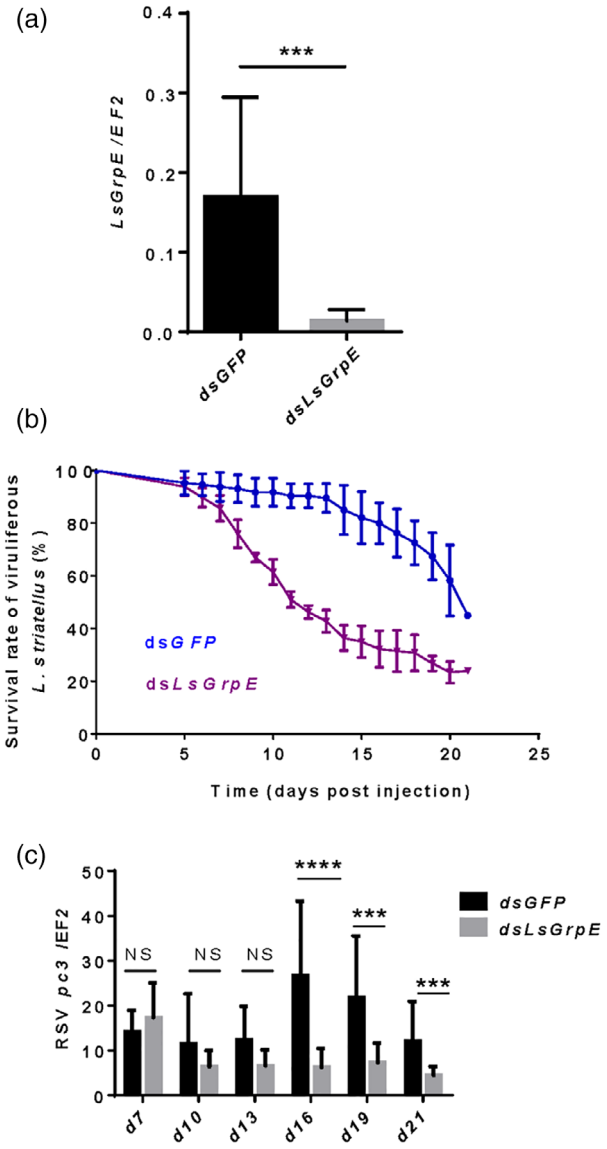

FIGURE 6 LsGrpE deficiency reduces the RSV titre in RSV-infected *L. striatellus*. (a) *LsGrpE* deficiency at 7 dpi. The mean and SD were calculated from three independent dsRNA injections, with six mRNA samples per experiment. ***, $p < 0.001$. (b) *L. striatellus* survival curves under LsGrpE deficiency. The figure shows representative data from four independently repeated experiments. (c) Q-RT-PCR to show the RSV titres in the ds*LsGrpE*-treated and ds*GFP*-treated *L. striatellus*. RSV titres were measured from 7 to 21 dpi. The RSV burden was shown as pc3 copies/SBPH ef2. *, $p < 0.05$; ****, $p < 0.0001$; *NS*, not significant

these two lines for 1 week, and then the transcript level of *LsGrpE* in the insects was determined. Compared with insects feeding on control plants, those feeding on GP1-5 and GP1-1 showed decreases in *LsGrpE* mRNA of more than 80%, indicating that feeding on transgenic plants led to silencing of *LsGrpE* expression in insects (Figure 7b). After 2 weeks of feeding, the survival rate was significantly lower in insects feeding on transgenic lines GP1-5 (65.77% ± 6.38%) and GP1-1 (62.95% ± 11.76%) than in those feeding on control plants (95% ± 5.59%) (Figure 7c).

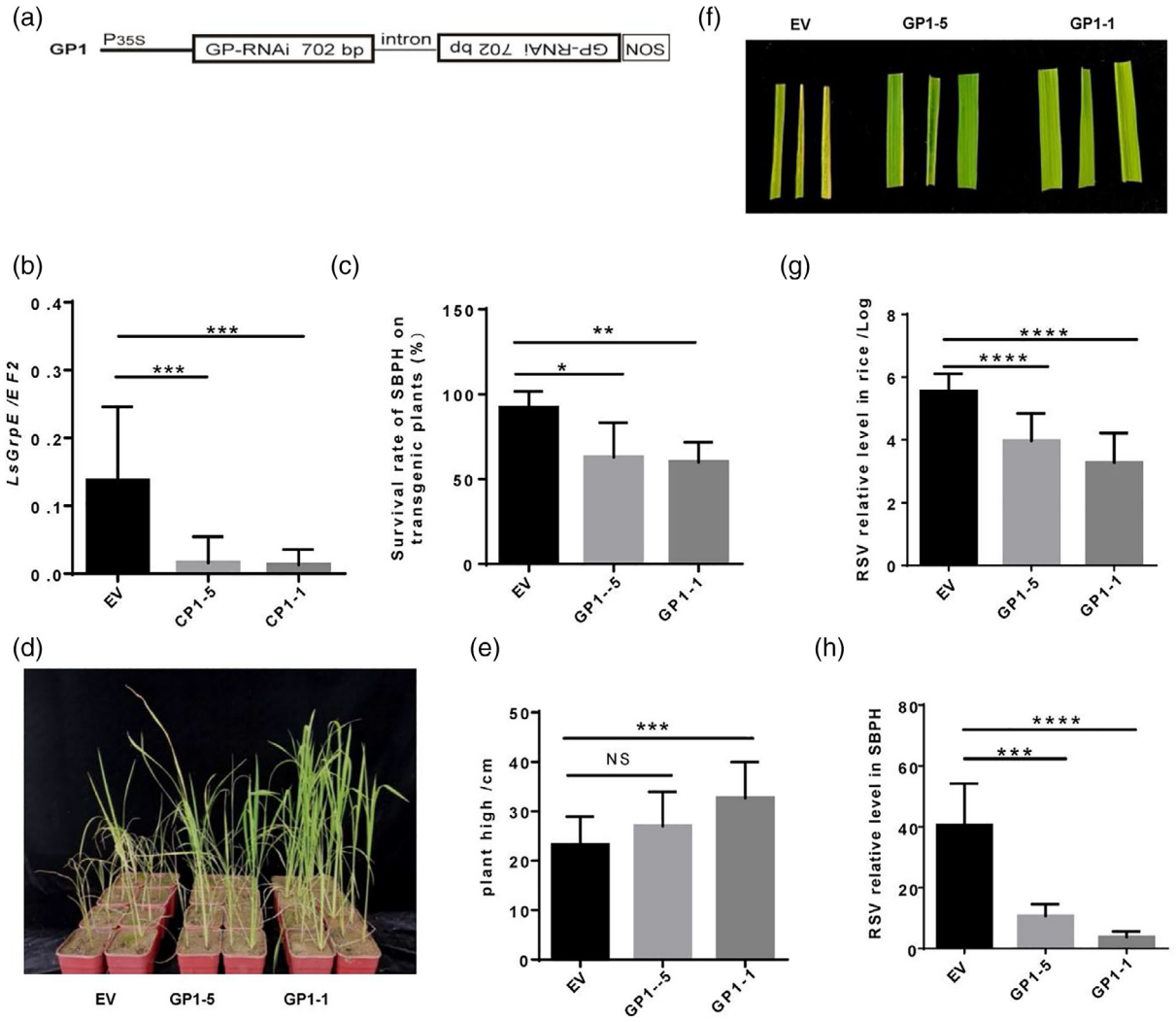

FIGURE 7 LsGrpE-RNAi transgenic rice is resistant to insects and RSV. (a) Construction of LsGrpE-hairpin-RNA target (GP1) overexpression transgenic plants. In the GP1 construct, a long fragment of hairpin ds-GrpE (705 bp) mediated by an intron was produced and delivered via the CaMV 35S constitutive promoter (P35S). (b,c) Resistance to *L. striatellus* of transgenic plants lines (GP1-1 and GP1-5). Plants with the empty-vector (EV) were a control. The *LsGrpE* transcript level was detected at 1 week post-feeding on different groups of plants (B) and the survival ratio was determined at 2 weeks post-feeding on different groups of plants (c). (d–h) Resistance to RSV of transgenic plants. Plants were treated with 90 viruliferous SBPHs (five viruliferous SBPHs per plant) for 1 month. The rates of RSV infection in different groups of plants were detected based on symptoms (d–f) and virus titre detection by q-RT-PCR (g, h). The results are the mean ± SD of three biological replicates with their respective three technical replicates. *, $p < 0.05$, **, $p < 0.01$, ***, $p < 0.001$, ****, $p < 0.0001$

To determine the antiviral activity of ds*LsGrpE* expressed in the transgenic plants, 90 RSV-infected *L. striatellus* were allowed to feed on 18 transgenic plants outdoors for 1 month, and then the viral load in the plants and insects was measured. The control plants showed severe symptoms of rice stripe disease, which included stripes on the leaves and withering of the whole plant. The GP1-5 and GP1-1 plants showed much milder symptoms of rice stripe disease, with stronger, taller plants and less pronounced stripes on the leaves. The symptoms were less severe in GP1-1 than in GP1-5 (Figure 7d–f). When the RSV titre was measured in these plants by q-RT-PCR, the viral load was significantly lower in GP1-1 and GP1-5 than in control plants (Figure 7g). In addition, the viral load in viruliferous *L. striatellus* was lower in insects feeding on GP1-1 and GP1-5 than in those feeding on control plants (Figure 7h). These results indicated that *LsGrpE* siRNA produced in plants can be acquired by insects during feeding, and can interfere with *LsGrpE* expression to decrease insect survival, and prevent RSV transmission.

DISCUSSION

In this study, we identified *L. striatellus GrpE* as a target gene for RNAi and produced rice plants expressing the *LsGrpE*-specific dsRNA to control this sap-feeding pest and the arbovirus RSV. We demonstrated that LsGrpE is a mitochondrial protein whose deficiency led to

mtD, resulting in an insufficient supply of ATP, excess ROS inside cells, defective blood sugar regulation, developmental delays, inactive behaviour, and significantly higher mortality. *LsGrpE* deficiency also affected RSV transmission. On the one hand, RSV titre in *LsGrpE*-deficient insects was dramatically reduced; on the other hand, because most *LsGrpE*-deficient insects are unable to moult into adults, vertical transmission of the virus was perturbed. By generating transgenic rice plants expressing *LsGrpE*-specific dsRNA, we demonstrated that *LsGrpE* is a suitable target in insects, and that its expression can be repressed by feeding on transgenic plants. In this way, we produced transgenic plants showing resistance to *L. striatellus* and RSV transmission.

LsGrpE deficiency had a delayed antiviral effect when compared with its anti-insect effect. LsGrpE deficiency delayed insect development by disturbing mitochondrial function. MtD may directly impact on the replicative capability of RSV or high levels of RSV infection may further damage insect health and development, while lower virus titres might offer self-protection against stress. In this study, when insects were infected by RSV, their survival rate under LsGrpE deficiency was significantly lower than that of the healthy insects (Figures 3b and 6b and Figure S3), indicating the double burden from both virus infection and LsGrpE deficiency. To measure the influence of RSV replication on *L. striatellus* development, we isolated RSV-free and RSV-infected *L. striatellus* ovaries for in vitro culture. We found that RSV can continue to replicate in the isolated ovarian tissues, and that ovarian development is much slower than in RSV-free ovaries (Figure S4), indicating the negative impact of RSV replication on insect development.

In this study, LsGrpE deficiency caused mtD, which led to the inhibition of ATP production and excessive ROS accumulation. Excessive ROS are considered to be the main cause of type 2 diabetes. In previous studies, mtD-induced disturbances in sugar metabolism have been reported in mammals and fruit flies (Kleinridders et al., 2013; Maechler & Wollheim, 2000; Sebastián et al., 2012). For example, in humans and rodents, impaired mitochondrial function inhibited insulin secretion in insulin-producing cells (Supale et al., 2013; Wang & Wei, 2020). The excessive production of ROS during mtD disrupted insulin signal transduction and downregulated sugar transporters, causing insulin resistance (Jing et al., 2011; Lantier et al., 2015). The insulin pathway can also affect development and lifespan. For example, insulin-resistant or diabetic flies exhibit abnormal developmental phenotypes (Rulifson et al., 2002; Zhang et al., 2009). Consistent with this, the main phenotypes of LsGrpE-deficient *L. striatellus* were reduced viability, growth defects, and delayed development.

With the rapid development of bioengineering technology, the breeding of transgenic plants resistant to agricultural pests and diseases has improved. Some chewing insects have been effectively controlled using such breeding methods (Bakhsh et al., 2020; Makkar et al., 2019). However, because sap-feeding insects have a limited feed intake and different feeding methods (Douglas, 2006), the development of transgenic plants resistant to these insects has lagged behind, and targeted strategies need to be considered. Gene-specific dsRNA can efficiently inhibit gene expression when delivered into insects through microinjection or artificial feeding, but only a few studies have reported the use of dsRNA-producing transgenic plants to silence gene expression (Mutti et al., 2008; Tian et al., 2021). In this study, the *LsGrpE*-RNAi transgenic plants showed high resistance to *L. striatellus* and RSV, with no detectable trade-off in terms of growth, indicating LsGrpE as a valuable target for the control of sap-feeding pests, and therefore, also their arboviruses.

EXPERIMENTAL PROCEDURES

Insects rearing and plant cultivation

The healthy and viruliferous *L. striatellus* used in this study were originally captured in Jiangsu Province, China, and were maintained in a glass incubator (Φ65 × 200 mm) in our laboratory. The insects were reared in glass chambers with five to six seedlings of rice (*O. sativa* cv. Nipponbare) per chamber.

Rice seeds were imbibed in tap water for 2 d, and sown on a mixed matrix (vermiculite:nutritive soil = 5:1 v/v) in glass containers, with four seeds per container. Each container was sealed with nylon mesh (150 μm mesh size) to allow ventilation, and the plants were watered from the top of the container. The plants were grown at 25°C under a 16-h light/8-h dark photoperiod.

To measure insect survival and development following LsGrpE deficiency, five insects were added to each container with 2-week-old rice seedlings, and their survival and development were monitored for 3 weeks. To test the RSV resistance of transgenic plants, 18 of the 4-week-old rice seedlings growing outdoors were exposed to 90 viruliferous *L. striatellus* (on average, five insects per plant) for 1 month at 20–30°C, and the insect survival and RSV infection rates were determined at the end of the 1-month period.

Mitochondria isolation and LsGrpE localization detection

To determine the mitochondrial localization of LsGrpE, the BioVision Mitochondria Isolation Kit (BioVision, Milpitas, CA, USA) was used to separate mitochondria from insect cells. Briefly, 0.5 g of whole insects was ground into a powder in liquid nitrogen, suspended in extraction buffer, then incubated for 30 min. After centrifugation at 600 × *g* at 4°C for 4 min, the supernatant was transferred to a new tube (total protein). The pellet was centrifuged again at 7000 × *g* at 4°C for 10 min, and the supernatant was transferred to another tube (cytoplasmic protein). The pellet was washed and resuspended in extraction buffer as the mitochondrial fraction. The separated samples were incubated with 0.1 ng/μL Mito-Tracker Red CMXRos for 10 min and imaged with a 40× objective lens under a Leica SP8 confocal microscope (Leica, Germany). The extracted proteins were fractionated by SDS-PAGE, and western blotting was performed with rabbit anti-LsGrpE polyclonal antibodies, which were produced against the LsGrpE-specific polypeptide HQALFDKEDEEKKPG.

Insect dissection and tissue collection

L. striatellus haemocytes, midgut, salivary glands, fat body, and ovary were isolated according to previously described protocols (Huo et al., 2018). Briefly, insects were anesthetised at 20°C for 3 min, and then the forelegs were severed at the coxa-trochanter joint using forceps. The haemolymph containing haemocytes was expelled and drawn to the tip of clean forceps. Only clear droplets were collected to avoid contamination of the fat body. The insects were then dissected in pre-chilled phosphate-buffered saline (PBS). Insects were dissected from the abdomen, and the wound was rinsed gently twice with PBS buffer. The white nubby fat body, without contamination from other tissues, was picked up by forceps with the help of the tension of the liquid and placed in PBS buffer. The midgut, salivary glands, and ovaries were washed twice with PBS to remove any contaminating viruses from the haemolymph.

Microinjection of dsRNA

To synthesize gene-specific dsRNA, the *LsGrpE* fragment was amplified from *L. striatellus* cDNA using gene-specific primer pairs with the T7-promoter (*LsGrpE-T7F/R*). Then, dsRNA was synthesized using the T7 RiboMAX Express RNAi System (Promega,USA) and purified by phenol-chloroform extraction and isopropanol precipitation. For gene silencing, the 3rd instar larvae were anaesthetised on ice and then injected with 36.8 nL of dsRNA (1 ng/nL) or *ds*GFP (negative control) into the hemocoel through a glass needle using a Nanoliter 2000 instrument (World Precision Instruments, USA), following our previously reported work (Huo et al., 2018). Each group of insects was reared separately in glass chambers.

Transcriptome sequencing and gene transcript analyses

The 3rd instar larvae were microinjected with *dsGFP* or *dsLsGrpE*. At 7 dpi, total RNA was extracted from every 10 insects using the RNeasy Mini Kit (QIAGEN, Germany) according to the manufacturer's instructions. Oligo (dT) beads were used to enrich mRNA. Then, the enriched mRNA was fragmented into short fragments using fragmentation buffer and reverse transcribed into cDNA with random primers. Second-strand cDNA was synthesized by DNA polymerase I in the presence of RNase H, dNTPs, and buffer. Then, the cDNA fragments were purified with the QiaQuick PCR extraction kit and end-repaired, followed by the addition of a poly(A)-tail and ligation to Illumina sequencing adapters. The ligation products were size selected by agarose gel electrophoresis, PCR amplified, and sequenced using Illumina HiSeq™ 2000 by Gene Denovo Biotechnology Co. (Guangzhou, China).

Two groups of insects were used for transcriptome sequencing analyses, including RSV-free insects treated with dsLsGrpE or dsGFP. Three sequencing samples were prepared for each group. Therefore, two groups of six samples were sequenced and analysed.

The raw reads were filtered to remove low-quality reads and ribosomal RNA to obtain high-quality clean reads, which were then mapped to the genomic sequence of *L. striatellus* (taxid: 195883) (Zhu et al., 2017) using the short reads alignment tool Bowtie2 under default parameters. The mapping ratio of each sample was higher than 70%. All samples expressed 42,085 genes, which was 95.02% of the number of reference genes. Each sample expressed more than 87% of the total reference genes.

To identify DEGs between groups, the edgeR package (http://www.r-project.org/) was used. We identified genes with a fold change ≥2 and a false discovery rate (FDR) <0.05 in a comparison of significant DEGs. DEGs were then subjected to enrichment analyses of GO functions and KEGG pathways.

For quantitative analyses of gene transcript levels in ds*GFP*- and ds*LsGrpE*-treated insects on 7 dpi, RNA was extracted using the RNeasy Mini Kit (QIAGEN, Germany). Reverse-transcription PCR (iScript cDNA Synthesis Kit, Bio-Rad, USA) and SYBR-Green-based qPCR (SYBR Green Supermix, Bio-Rad) were performed according to the manufacturer's protocols. The gene-specific primer pairs used for gene amplification were LsGrpE-q-F/R; RFT-q-F/R; CAML-q-F/R; TFKI–q-F/R; GGCT-q-F/R; CEBPβ-q-F/R; LsImpL2-q-F/R; IS1-q-F/R; IS3-q-F/R; IS4-q-F/R; ISR1-q-F/R; and ISR2-q-F/R. The RSV level was tested using Pc3-q-F/R. To normalize gene transcript levels in *L. striatellus*, the transcript level of translation elongation factor 2 (EF2) was determined using the primer pair ef2-q-F/R. For gene expression analyses in rice, the *O. sativa actin* gene was used for normalization, and was amplified with actin-q-F/R primers. All primer sequences are listed in Table S3. The relative levels of genes in SBPH or rice were calculated according to the formula $2^{Ct\ (EF2)Ct\ (target\ gene)}$ or $2^{\ Ct\ (actin)Ct\ (target\ gene)}$, respectively.

ATP assay

The ATP level in *L. striatellus* was determined following the standard protocol of the ATP content assay kit (Cat #AKOP004M, Boxbio, China). Hexokinase can catalyse the synthesis of glucose 6-phosphate from glucose and ATP. Glucose 6-phosphate dehydrogenase further catalyses the dehydrogenation of glucose 6-phosphate to NADPH. NADPH has a characteristic absorption peak at 340 nm. The ATP content can be quantitatively detected by measuring the change in absorbance at 340 nm. For each sample, two insects were homogenized in ATP extraction buffer. After centrifugation at 10,000 × *g* for 10 min, the supernatant was collected and extracted with chloroform. Then, 200 μL of the extract was used for an ATP content assay. The samples, as well as a standard sample (0.625 μmol/mL ATP in ddH_2O), were incubated with the working buffer (containing hexokinase, glucose, glucose dehydrogenase, and NADP). At 10 and 190 s after incubation, the absorbance of the synthesized NADPH was detected by a microplate reader at 340 nm. The ATP contents (μmol/g) of the samples are calculated by comparison with the standard sample. A total of six biological replicates were performed, each of which included three technical replicates.

Dihydroethidium staining

The midgut and fat body were dissected from *L. striatellus* in medium. Immediately after dissection, the midgut was incubated with 10 μM dihydroethidium (DHE, for ROS staining) and 5 μM Hoechst 33342 (for nuclear staining) in medium at room temperature for 30 min in the dark. Then, the tissues were washed three times with PBS. Slides were imaged using a 20× objective lens under a Leica SP8 confocal microscope (Leica, Germany) in multi-track mode.

Test of circulating sugar

Monosaccharides were quantified using a Boxbio trehalose detection kit (Boxbio, China). Haemolymph (0.2 μL, collected from 10 insects) was diluted with 9.8 μL PBS, then the mixture was centrifuged at 3000 × *g* for 10 min. The cell sediment was discarded and the supernatant was diluted 10-fold in extraction buffer from the kit. The mixture was incubated for 45 min at room temperature, then centrifuged at 8000 × *g* for 10 min. The supernatant was collected and the sediment was discarded. Then, 10 μL of diluted sample and the standard sample were each incubated with chromogenic substrate at 95°C for 10 min. The fluorescence intensity was measured at an excitation wavelength of 620 nm. The monosaccharide concentration was determined by comparison with a standard curve.

Bioinformatics and phylogenetic analyses

The signal peptide of LsGrpE was predicted through the TargetP-1.1 server (https://services.healthtech.dtu.dk/service.php?TargetP-1.1). Homology searches of the protein sequence of LsGrpE were conducted using the BLAST algorithm at the National Center for Biotechnology Information (http://blast.ncbi. nlm.nih.gov/Blast.cgi). Multiple sequence alignments of LsGrpE and other GrpEs were performed using the CLUSTALW program (http://www.ch.embnet.org/software/ClustalW.html). The phylogenetic tree was constructed based on the deduced amino acid sequence of LsGrpE and other GrpEs using the neighbour-joining method (Saitou & Nei, 1987). The optimal tree with the sum of branch length = 10.78796588 is shown. The tree is drawn to scale, with branch lengths in the same units as those of the evolutionary distances used to infer the phylogenetic tree. The evolutionary distances were computed using the Poisson correction method (Zuckerkandl & Pauling, 1965) and are in the units of the number of amino acid differences per site. These analyses involved 47 amino acid sequences. All positions containing gaps and missing data were eliminated. There were a total of 133 positions in the final dataset. Evolutionary analyses were conducted in MEGA6 (Tamura et al., 2013).

Before constructing RNAi transgenic plants, *LsGrpE* homologous sequences were searched for among the human (taxid: 9606), *Japonica* rice (taxid: 39947), cow (taxid: 9913), sheep (taxid: 9940), and leafhopper (taxid: 30102) genomes, using NCBI Blast. Because ds*LsGrpE* would be cleaved into various siRNAs of 20–24 base pairs, we set the "word size" parameter of the BLAST tool on the NCBI website to 20 and 24, and the Expect threshold to 10. For other general parameters, the default settings of the software were used.

Construction of RNAi expression plasmids

The RNAi technique was used to produce transgenic plants overexpressing a dsRNA fragment targeting a gene that is essential for *L. striatellus* development. A hairpin RNA (hpRNA) was produced (Figure 7) using a previously reported method (Zhang et al., 2012). To make the hpRNA, we generated an intron-spliced self-complementary construct GPab-RNAi that contained the sense and antisense sequences of a 705-bp *LsGrpE*-cDNA region. Both fragments were amplified from *L. striatellus* using the primer pairs GPa-Eco/GPa-kpn and GPb-Bam/GPb-Xba, respectively. The two fragments were further cloned into the plant expression vector pCAMBIA-HAN via *EcoR* I/*Kpn* I and *Bam* HI/*Xba* I double restriction enzyme sites, respectively, to create an RNAi vector GPab-RNAi (designated as GP1).

The recombinant construct was transformed into the *Japonica* rice cultivar Nipponbare using *Agrobacterium*-mediated transformation protocols as described previously (Hiei et al., 1994). For each construct, approximately 30 independent T_0 transformants were obtained. The transformants were further screened by germinating seeds from T_2 lines on medium containing 50 μg/mL hygromycin. The hygromycin-resistant homozygous seeds were used for further experiments. Seeds from homozygous lines transformed with the empty vector pCAMBIA 1300 were used as a negative control.

Statistical analyses

All graphing and statistical analyses were performed using Prism 6.0 software (GraphPad Software, CA, USA). Data were expressed as means ± standard deviations (SD). The significance of differences between two groups was evaluated using Student's t-test, and the significance of differences between more groups was evaluated by one-way ANOVA.

ACKNOWLEDGMENTS

This work was supported by the Strategic Priority Research Program of the Chinese Academy of Sciences (Grant No. XDPB16), the National Key Research and Development Program of China (No. 2019YFC1200503), and the Youth Innovation Promotion Association CAS (2021084).

CONFLICT OF INTEREST

The authors declare no conflict of interest.

AUTHOR CONTRIBUTIONS

Lili Zhang, Yuman Zhang, Yan Huo, and Rongxiang Fang designed the experiments. Yan Huo, Yuman Zhang, Haiting Wang, Ziyu Zhang, and Na Xiao performed the experiments. Yan Huo, Yuman Zhang, and

Yuman Zhang analysed the results. Lili Zhang, Yuman Zhang, and Yan Huo wrote the manuscript.

DATA AVAILABILITY STATEMENT

Data openly available in a public repository that issues datasets with DOIs.

ORCID

Yan Huo https://orcid.org/0000-0002-5783-1708
Rongxiang Fang https://orcid.org/0000-0002-1677-4591
Yuman Zhang https://orcid.org/0000-0002-9616-0206
Lili Zhang https://orcid.org/0000-0002-4321-0521

REFERENCES

Bakhsh, A., SDD, M., Naeem, M.H.A. & Yasmeen, A. (2020) Genetic approaches for engineering biotic stress resistance in potato (*Solanum Tuberosum* L.). *The Journal of Animal and Plant Sciences*, 30, 1–17.

Bhattacharya, S. (2019) Brassica-aphid interaction: challenges and prospects of genetic engineering for integrated aphid management. *Physiological and Molecular Plant Pathology*, 108, 101442.

Clavier, A., Rincheval-Arnold, A., Colin, J., Mignotte, B. & Guénal, I. (2016) Apoptosis in drosophila: which role for mitochondria? *Apoptosis*, 21, 239–251.

Coyne, L.P. & Chen, X.J. (2019) Consequences of inner mitochondrial membrane protein misfolding. *Mitochondrion*, 49, 46–55.

Douglas, A.E. (2006) Phloem-sap feeding by animals: problems and solutions. *Journal of Experimental Botany*, 57, 747–754.

Fang, X., Bogomolovas, J., Wu, T., Zhang, W., Liu, C., Veevers, J. et al. (2017) Loss-of-function mutations in co-chaperone BAG3 destabilize small HSPs and cause cardiomyopathy. *The Journal of Clinical Investigation*, 127, 3189–3200.

Guo, H., Song, X., Xie, C., Huo, Y., Zhang, F., Chen, X. et al. (2013) Rice yellow stunt rhabdovirus protein 6 suppresses systemic RNA silencing by blocking RDR6-mediated secondary siRNA synthesis. *Molecular Plant-Microbe Interactions*, 26, 927–936.

Han, S.H., Kim, J.H., Kim, K. & Lee, S.H. (2019) Selection of lethal genes for ingestion RNA interference against western flower thrips, Frankliniella occidentalis, via leaf disc-mediated dsRNA delivery. *Pesticide Biochemistry and Physiology*, 161, 47–53.

Hartl, F.U., Bracher, A. & Hayer-Hartl, M. (2011) Molecular chaperones in protein folding and proteostasis. *Nature*, 475, 324–332.

Hiei, Y., Ohta, S., Komari, T. & Kumashiro, T. (1994) Efficient transformation of rice (Oryza sativa L.) mediated by agrobacterium and sequence analysis of the boundaries of the T-DNA. *The Plant Journal*, 6, 271–282.

Hogenhout, S.A., Ammar, E.-D., Whitfield, A.E. & Redinbaugh, M.G. (2008) Insect vector interactions with persistently transmitted viruses. *Annual Review of Phytopathology*, 46, 327–359.

Huo, Y., Liu, W., Zhang, F., Chen, X., Li, L., Liu, Q. et al. (2014) Transovarial transmission of a plant virus is mediated by vitellogenin of its insect vector. *PLoS Pathogens*, 10, e1003949.

Huo, Y., Yu, Y., Chen, L., Li, Q., Zhang, M., Song, Z. et al. (2018) Insect tissue-specific vitellogenin facilitates transmission of plant virus. *PLoS Pathogens*, 14, e1006909.

Huo, Y., Yu, Y., Liu, Q., Liu, D., Zhang, M., Liang, J. et al. (2019) Rice stripe virus hitchhikes the vector insect vitellogenin ligand-receptor pathway for ovary entry. *Philosophical Transactions of the Royal Society of London. Series B, Biological Sciences*, 374, 20180312.

Jing, E., Emanuelli, B., Hirschey, M.D., Boucher, J., Lee, K.Y., Lombard, D. et al. (2011) Sirtuin-3 (Sirt3) regulates skeletal muscle metabolism and insulin signaling via altered mitochondrial oxidation and reactive oxygen species production. *Proceedings of the National Academy of Sciences of the United States of America*, 108, 14608–14613.

Kim, K., Kim, M.J., Han, S.H., Kim, S.H., Kim, J.H. & Lee, S.H. (2019) Amount and time course of ingestion of plant subcellular fractions by two thrips and one reference mite species. *Journal of Asia-Pacific Entomology*, 22, 733–736.

Kleinridders, A., Lauritzen, H.P., Ussar, S., Christensen, J.H., Mori, M.A., Bross, P. et al. (2013) Leptin regulation of Hsp60 impacts hypothalamic insulin signaling. *The Journal of Clinical Investigation*, 123, 4667–4680.

Konovalova, S., Liu, X., Manjunath, P., Baral, S., Neupane, N., Hilander, T. et al. (2018) Redox regulation of GRPEL2 nucleotide exchange factor for mitochondrial HSP70 chaperone. *Redox Biology*, 19, 37–45.

Langner, U., Baudisch, B. & Klösgen, R.B. (2014) Organelle import of proteins with dual targeting properties into mitochondria and chloroplasts takes place by the general import pathways. *Plant Signaling & Behavior*, 9, e29301.

Lantier, L., Williams, A.S., Williams, I.M., Yang, K.K., Bracy, D.P., Goelzer, M. et al. (2015) SIRT3 is crucial for maintaining skeletal muscle insulin action and protects against severe insulin resistance in high-fat-fed mice. *Diabetes*, 64, 3081–3092.

Liu, X.D., Zhai, B.P. & Liu, C.M. (2006) Outbreak reasons of *Laodelphax striatellus* population. *Chinese Bulletin of Entomology*, 43(2), 141–146.

Maechler, P. & Wollheim, C.B. (2000) Mitochondrial signals in glucose-stimulated insulin secretion in the beta cell. *The Journal of Physiology*, 529(Pt 1), 49–56.

Makkar, G.S., Bhatia, D., Suri, K.S. & Kaur, S. (2019) Insect resistance in Rice (*Oryza sativa* L.): overview on current breeding interventions. *International Journal of Tropical Insect Science*, 39, 259–272.

Marada, A., Allu, P.K., Murari, A., PullaReddy, B., Tammineni, P., Thiriveedi, V.R. et al. (2013) Mge1, a nucleotide exchange factor of Hsp70, acts as an oxidative sensor to regulate mitochondrial Hsp70 function. *Molecular Biology of the Cell*, 24, 692–703.

Melero, R., Moro, F., Pérez-Calvo, M., Perales-Calvo, J., Quintana-Gallardo, L., Llorca, O. et al. (2015) Modulation of the chaperone DnaK allosterism by the nucleotide exchange factor GrpE. *The Journal of Biological Chemistry*, 290, 10083–10092.

Mottis, A., Jovaisaite, V. & Auwerx, J. (2014) The mitochondrial unfolded protein response in mammalian physiology. *Mammalian Genome*, 25, 424–433.

Mutti, N.S., Louis, J., Pappan, L.K., Pappan, K., Begum, K., Chen, M.S. et al. (2008) A protein from the salivary glands of the pea aphid, *Acyrthosiphon pisum*, is essential in feeding on a host plant. *Proceedings of the National Academy of Sciences of the United States of America*, 105, 9965–9969.

Nunnari, J. & Suomalainen, A. (2012) Mitochondria: in sickness and in health. *Cell*, 148, 1145–1159.

Pfanner, N., Warscheid, B. & Wiedemann, N. (2019) Mitochondrial proteins: from biogenesis to functional networks. *Nature Reviews. Molecular Cell Biology*, 20, 267–284.

Rulifson, E.J., Kim, S.K. & Nusse, R. (2002) Ablation of insulin-producing neurons in flies: growth and diabetic phenotypes. *Science*, 296, 1118–1120.

Saitou, N. & Nei, M. (1987) The neighbor-joining method: a new method for reconstructing phylogenetic trees. *Molecular Biology and Evolution*, 4, 406–425.

Sebastián, D., Hernández-Alvarez, M.I., Segalés, J., Sorianello, E., Muñoz, J.P., Sala, D. et al. (2012) Mitofusin 2 (Mfn2) links mitochondrial and endoplasmic reticulum function with insulin signaling and is essential for normal glucose homeostasis. *Proceedings of the National Academy of Sciences of the United States of America*, 109, 5523–5528.

Supale, S., Thorel, F., Merkwirth, C., Gjinovci, A., Herrera, P.L., Scorrano, L. et al. (2013) Loss of prohibitin induces mitochondrial damages

altering β-cell function and survival and is responsible for gradual diabetes development. *Diabetes*, 62, 3488–3799.
Tamura, K., Stecher, G., Peterson, D., Filipski, A. & Kumar, S. (2013) MEGA6: molecular evolutionary genetics analysis version 6.0. *Molecular Biology and Evolution*, 30, 2725–2729.
Tian, T., Ji, R., Fu, J., Li, J., Wang, L., Zhang, H. et al. (2021) A salivary calcium-binding protein from *Laodelphax striatellus* acts as an effector that suppresses defense in rice. *Pest Management Science*, 77, 2272–2281.
Wang, C.H. & Wei, Y.H. (2020) Roles of mitochondrial Sirtuins in mitochondrial function, redox homeostasis, insulin resistance and type 2 diabetes. *International Journal of Molecular Sciences*, 21(15), 5266.
Xia, J., Guo, Z., Yang, Z., Han, H., Wang, S., Xu, H. et al. (2021) Whitefly hijacks a plant detoxification gene that neutralizes plant toxins. *Cell*, 184, 1693–1705.e17.
Yoneda, T., Benedetti, C., Urano, F., Clark, S.G., Harding, H.P. & Ron, D. (2004) Compartment-specific perturbation of protein handling activates genes encoding mitochondrial chaperones. *Journal of Cell Science*, 117, 4055–4066.
Zhang, H., Liu, J., Li, C.R., Momen, B., Kohanski, R.A. & Pick, L. (2009) Deletion of drosophila insulin-like peptides causes growth defects and metabolic abnormalities. *Proceedings of the National Academy of Sciences of the United States of America*, 106, 19617–19622.
Zhang, Y., Li, Z.X., Yu, X.D., Fan, J., Pickett, J.A., Jones, H.D. et al. (2015) Molecular characterization of two isoforms of a farnesyl pyrophosphate synthase gene in wheat and their roles in sesquiterpene synthesis and inducible defence against aphid infestation. *The New Phytologist*, 206, 1101–1115.
Zhang, Y.M., Yan, Y.S., Wang, L.N., Yang, K., Xiao, N., Liu, Y.F. et al. (2012) A novel rice gene, NRR responds to macronutrient deficiency and regulates root growth. *Molecular Plant*, 5, 63–72.
Zhu, J., Jiang, F., Wang, X., Yang, P., Bao, Y., Zhao, W. et al. (2017) Genome sequence of the small brown planthopper, Laodelphax striatellus. *Gigascience*, 6, 1–12.
Zuckerkandl, E. & Pauling, L. (1965) Evolutionary divergence and convergence in proteins. In: Bryson, V. & Vogel, H.J. (Eds.) *Evolving Genes and Proteins*. USA: Academic Press, pp. 97–166.

SUPPORTING INFORMATION

Additional supporting information may be found in the online version of the article at the publisher's website.

Figure S1 Directed acyclic graph of GO enrichment analyses and DEG functional annotation. Circles and rectangles represent GO terms, the upstream GO term includes the downstream GO terms (arrows) and the colour represents the degree of GO function enrichment. A darker colour indicates greater enrichment of the term. The name and *p*-value of each term are present on the node. DEGs, differentially expressed genes; GO, gene ontology.

Figure S2 Survival rate of *Laodelphax striatellus* when fed on transgenic and wild-type rice seedlings. From GP1-1 to GP1-8, the transgenic plant lines; EV, plants transformed with the empty vector. The survival rate was calculated from the insects fed on plants for 2 weeks. **, $p < 0.01$.

Figure S3 Survival curves to show the effect of LsGrpE deficiency (dsLsGrpE) on insect survival. dsGFP was used as a negative control. V, RSV-free insects; V+, viruliferous insects.

Figure S4 RSV titre in the medium-cultured ovaries. Ovaries were dissected from RSV-infected female *L. striatellus* 48 h after eclosion and were incubated in medium for 2 days. RSV titre (A) and EF2 mRNA level (B) were measured through q-RT-PCR. Results are the mean ± SD of four biological replicates. **, $p < 0.01$.

Table S1 The differentially expressed genes identified through transcriptome sequencing of the *dsGFP* and *dsLsGrpE*-treated *L. striatellus*

Table S2 Genes related to mitochondrial function and the response to mitochondrial dysfunction

Table S3 Primers used in this study

How to cite this article: Huo, Y., Song, Z., Wang, H., Zhang, Z., Xiao, N., Fang, R. et al. (2022) GrpE is involved in mitochondrial function and is an effective target for RNAi-mediated pest and arbovirus control. *Insect Molecular Biology*, 31(3), 377–390. Available from: https://doi.org/10.1111/imb.12766